

# Transient radiative hydromagnetic free convection flow past an impulsively started vertical plate with uniform heat and mass flux

V.Ramachandra Prasad \*      N.Bhaskar Reddy †  
R.Muthucumaraswamy ‡

## Abstract

The interaction of free convection with thermal radiation of viscous incompressible MHD unsteady flow past an impulsively started vertical plate with uniform heat and mass flux is analyzed. This type of problem finds application in many technological and engineering fields such as rocket propulsion systems, space craft re-entry aerothermodynamics, cosmical flight aerodynamics, plasma physics, glass production and furnace engineering .The Rosseland approximation is used to describe the radiative heat transfer in the limit of the optically thin fluid. The non-linear, coupled equations are solved using an implicit finite difference scheme of Crank-Nicolson type. Velocity, temperature and concentration of the flow have been presented for various parameters such as thermal Grashof number, mass Grashof number, Prandtl number, Schmidt number, radiation parameter and magnetic parameter. The local and average skin friction, Nusslet number and Sherwood number are also presented graphically. It is observed that, when the radiation parameter increases the velocity and temperature decrease in the boundary layer.

**Keywords:** Radiation, heat and mass transfer, MHD.

---

\*Department of Mathematics, Sri Venkateswara University Tirupati-517502, India,  
e-mail: rcpmaths@gmail.com

†Department of Mathematics, Sri Venkateswara University Tirupati-517502, India

‡Department of Information Technology Sri Venkateswara College of Engineering Sri  
Perumbudur-602105, India

**List of symbols**

$B_0$	magnetic field strength
$c_p$	specific heat
$C'$	concentration
$C$	dimensionless concentration
$D$	mass diffusion coefficient
$g$	acceleration due to gravity
$Gm$	mass Grashof number
$Gr$	thermal Grashof number
$k$	thermal conductivity
$L$	reference length
$M$	magnetic parameter
$N$	conduction-radiation
$Nu_X$	dimensionless local Nusselt Number
$\overline{Nu}$	dimensionless average Nusselt number
$Pr$	Prandtl number
$q_r$	radiative heat flux
$q'_w$	heat flux per unit area at the plate
$q_w^*$	mass flux per unit area
$Sc$	Schmidt number
$Sh_X$	dimensionless local Sherwood number
$\overline{Sh}$	dimensionless average Sherwood number
$T'$	temperature
$T$	dimensionless temperature
$t'$	time
$t$	dimensionless time
$u_0$	velocity of the plate
$u, v$	velocity components in $x, y$ -directions respectively
$U, V$	dimensionless velocity components in $X, Y$ -directions respectively
$x$	spatial coordinate along the plate
$X$	dimensionless spatial coordinate along the plate
$y$	spatial coordinate normal to the plate
$Y$	dimensionless spatial coordinate normal to the plate

**Greek symbols**

$\alpha$	thermal diffusivity
$\beta$	volumetric coefficient of thermal expansion
$\beta^*$	volumetric coefficient of expansion with concentration
$\sigma$	electrical conductivity parameter
$\nu$	kinematic viscosity
$\rho$	density
$\tau_X$	dimensionless local skin-friction
$\bar{\tau}$	dimensionless average skin-friction

### Subscripts

$w$	conditions on the wall
$\infty$	free stream conditions

## Introduction

Stokes [1] first presented an exact solution to the Navier-Stokes equation, which for the flow of viscous incompressible fluid past an impulsively started infinite horizontal plate in its own plane. It is often called Rayleigh problem in the literature. Such a flow past an impulsively started semi-infinite horizontal plate was first presented by Stewartson [2]. Hall [3] considered the flow past an impulsively started semi-infinite horizontal plate by finite-difference method of explicit-implicit type. Following Stokes analysis Soundalgekar [4] was the first to present an exact solution to the flow of a viscous fluid past an impulsively started semi-infinite isothermal vertical plate. The solution was derived by the Laplace transform technique and the effects of heating or cooling of the plate on the flow field was discussed through Grashof number. Soundalgekar and Patil [5] have studied Stokes problem for an infinite vertical plate with constant heat flux. Muthucumaraswamy and Ganesan [6] studied first order chemical reaction on flow past an impulsively started vertical plate with uniform heat and mass flux.

Free convection flow occurs frequently in nature. It occurs not only due to temperature difference, but also due to concentration difference or

combination of these two, e.g., in atmospheric flows, there exists differences in the  $H_2O$  concentration and hence the flow is affected by such concentration difference. Flows in bodies of water are driven through the comparable effects upon density, of temperature, concentration of dissolved materials and suspended particulate matter. Many transport process exist in nature and in industrial applications in which the simultaneous heat and mass transfer occur as a result of combined buoyancy effects of diffusion of chemical species. A few representative fields of interest in which combined heat and mass transfer plays an important role of design of chemical process in equipment, formation and dispersion of fog, distribution of temperature and moisture over agriculture fields and groves of fruit trees, damage of crops due to freezing and the pollution of the environment. In this context Soundalgekar [7] extended his own problem of [5] to mass transfer effects.

The study of magnetohydrodynamics (MHD) plays an important role in agriculture, engineering and petroleum industries. The problem of free convection under the influence of a magnetic field has attracted the interest of many researchers in view of its applications in geophysics and astrophysics. Magnetohydrodynamics has its own practical applications. For instance, it may be used to deal with problems such as cooling of nuclear reactors by liquid sodium and induction flow meter, which depends on the potential difference in the fluid in the direction perpendicular to the motion and go the magnetic field. Soundalgekar et al. [8] analysed the problem of free convection effects on Stokes problem for a vertical plate under the action of transversely applied magnetic field. Elbashbeshy [9] studied the heat and mass transfer along a vertical plate under the combined buoyancy effects of thermal and species diffusion, in the presence of magnetic field. Helmy [10] presented an unsteady two-dimensional laminar free convection flow of an incompressible, electrically conducting (Newtonian or polar) fluid through a porous medium bounded by infinite vertical plane surface of constant temperature.

In the context of space technology and in processes involving high temperatures the effects of radiation are of vital importance. Recent developments in hypersonic flights, missile reentry, rocket combustion chambers, power plants for inter planetary flight and gas cooled nuclear reactors, have focused attention on thermal radiation as a mode of energy transfer, and emphasize the need for improved understanding of radiative transfer in these process. The interaction of radiation with laminar free convection

heat transfer from a vertical plate was investigated by Cess [11] for an absorbing, emitting fluid in the optically thick region, using the singular perturbation technique. Arpaci [12] considered a similar problem in both the optically thin and optically thick regions and used the approximate integral technique and first-order profiles to solve the energy equation. Cheng and Ozisik [13] considered a related problem for an absorbing, emitting and isotropically scattering fluid, and treated the radiation part of the problem exactly with the normal-mode expansion technique. Raptis [14] has analyzed the thermal radiation and free convection flow through a porous medium by using perturbation technique. Hossain and Takhar [15] studied the radiation effects on mixed convection along a vertical plate with uniform surface temperature using Keller Box finite difference method. In all these papers the flow is considered to be steady. The unsteady flow past a moving plate in the presence of free convection and radiation were studied by Mansour [16]. Raptis and Perdakis [17] studied the effects of thermal radiation and free convective flow past moving plate. Das et al. [18] have analyzed the radiation effects on flow past an impulsively started infinite isothermal vertical plate. Chamkha et al [19] et al studied the effect of radiation on free convective flow past a semi-infinite vertical plate with mass transfer. Ganesan and Loganathan [20] studied the radiation and mass transfer effects on flow of incompressible viscous fluid past a moving vertical cylinder using Rosseland approximation.

The objective of the present paper is to study unsteady, laminar, hydromagnetic simultaneous free convective heat and mass transfer flow along an impulsively started plate with uniform heat and mass flux in the presence of thermal radiation effects. The solution of the problem is obtained by using an implicit finite difference method of Crank-Nicolson type.

## Mathematical Analysis:

Consider a two-dimensional, transient, hydromagnetic, laminar natural convection flow of an incompressible viscous radiating fluid past an impulsively started semi-infinite vertical plate. It is assumed that the concentration  $C'$  of the diffusing species in the binary mixture is very less in comparison to the other chemical species, which are present. This leads to the assumption that the Soret and Dufour effects are negligible. It is

also assumed that the effect of viscous dissipation is negligible in the energy equation. The x-axis is taken along the plate in the upward direction the y-axis is taken normal to it. The plate starts moving impulsively in the vertical direction with constant velocity  $u_0$  and the temperature of the plate and the concentration level near the plate is also raised. Initially, it is assumed that the plate and the fluid are of the same temperature and concentration. The x-axis is taken along the plate in the upward direction the y-axis is taken normal to it. Initially, it is assumed that the plate and the fluid are of the same temperature and concentration in a stationary condition. At time  $t' > 0$ , the plate starts moving impulsively in the vertical direction with constant velocity  $u_0$  against the gravitational field. The temperature and concentration level near the plate are raised at a constant rate. Then under usual Boussinesq's approximation the unsteady flow past the semi-infinite vertical plate is governed by the following equations.

$$\frac{\partial u}{\partial x} + \frac{\partial v}{\partial y} = 0 \quad (1)$$

$$\frac{\partial u}{\partial t'} + u \frac{\partial u}{\partial x} + v \frac{\partial u}{\partial y} = g \beta (T' - T'_\infty) + g \beta^* (C' - C'_\infty) + \nu \frac{\partial^2 u}{\partial y^2} - \frac{\sigma B_0^2}{\rho} u \quad (2)$$

$$\frac{\partial T'}{\partial t'} + u \frac{\partial T'}{\partial x} + v \frac{\partial T'}{\partial y} = \alpha \frac{\partial^2 T'}{\partial y^2} - \frac{1}{\rho c_p} \frac{\partial q_r}{\partial y} \quad (3)$$

$$\frac{\partial C'}{\partial t'} + u \frac{\partial C'}{\partial x} + v \frac{\partial C'}{\partial y} = D \frac{\partial^2 C'}{\partial y^2} \quad (4)$$

The initial boundary conditions are

$$t' \leq 0 : u = 0, \quad v = 0, \quad T' = T'_\infty,$$

$$C' = C'_\infty t' > 0 : u = u_0, \quad v = 0,$$

$$\frac{\partial T'}{\partial y} = -\frac{q'_w(x)}{k}, \quad \frac{\partial C'}{\partial y} = -\frac{q_w^*(x)}{D} \quad \text{at } y = 0$$

$$\begin{aligned}
u &= 0, \quad T' = T'_\infty, \quad C' = C'_\infty \quad \text{at} \quad x = 0 \\
u &\rightarrow 0, \quad T' \rightarrow T'_\infty, \quad C' \rightarrow C'_\infty \quad \text{as} \quad y \rightarrow \infty
\end{aligned} \tag{5}$$

We now assume Rosseland approximation (Brewster [21]), which leads to the radiative heat flux  $q_r$  is given by

$$q_r = -\frac{4\sigma^*}{3\kappa^*} \frac{\partial T'^4}{\partial y} \tag{6}$$

where  $\sigma^*$  is the Stefan-Boltzmann constant and  $\kappa^*$  is the mean absorption coefficient.

If temperature differences within the flow are sufficiently small such that  $T'^4$  may be expressed as a linear function of the temperature, then the Taylor series for  $T'^4$  above  $T'_\infty$ , after neglecting higher order terms, is given by

$$T'^4 \cong 4T'^3_\infty T' - 3T'^4_\infty \tag{7}$$

In view of Eqs. (6) and (7), Eq. (3) reduces to

$$\frac{\partial T'}{\partial t'} + u \frac{\partial T'}{\partial x} + v \frac{\partial T'}{\partial y} = \alpha \frac{\partial^2 T'}{\partial y^2} + \frac{16\sigma T'^3_\infty}{3\kappa^* \rho c_p} \frac{\partial^2 T'}{\partial y^2} \tag{8}$$

On introducing the following non-dimensional quantities:

$$\begin{aligned}
X &= \frac{x u_0}{v}, \quad Y = \frac{y u_0}{v}, \quad t = \frac{t' u_0^2}{v}, \\
U &= \frac{u}{u_0}, \quad V = \frac{v}{u_0}, \quad Gr = \frac{g \beta q'_w v^2}{k u_0^4}, \\
Gm &= \frac{g \beta^* v^2 q'_w}{D u_0^4}, \quad N = \frac{\kappa^* k}{4\sigma T'^3_\infty}, \quad M = \frac{\sigma B_0^2 \nu}{u_0^2} \\
T &= \frac{T' - T'_\infty}{\left(\frac{q'_w v}{k u_0}\right)}, \quad C = \frac{C' - C'_\infty}{\left(\frac{q'_w v}{D u_0}\right)}, \quad Pr = \frac{\nu}{\alpha}, \quad Sc = \frac{\nu}{D}
\end{aligned} \tag{9}$$

Equations (1), (2), (3) and (4) are reduced to the following non-dimensional form

$$\frac{\partial U}{\partial X} + \frac{\partial V}{\partial Y} = 0 \quad (10)$$

$$\frac{\partial U}{\partial t} + U \frac{\partial U}{\partial X} + V \frac{\partial U}{\partial Y} = Gr T + Gm C + \frac{\partial^2 U}{\partial Y^2} - MU \quad (11)$$

$$\frac{\partial T}{\partial t} + U \frac{\partial T}{\partial X} + V \frac{\partial T}{\partial Y} = \frac{1}{Pr} \left( 1 + \frac{4}{3N} \right) \frac{\partial^2 T}{\partial Y^2} \quad (12)$$

$$\frac{\partial C}{\partial t} + U \frac{\partial C}{\partial X} + V \frac{\partial C}{\partial Y} = \frac{1}{Sc} \frac{\partial^2 C}{\partial Y^2} \quad (13)$$

The initial and boundary conditions are

$$\begin{aligned} t \leq 0 : U = 0, \quad V = 0, \quad T = 0, \quad C = 0, \\ t > 0 : U = 1, \quad V = 0, \quad \frac{\partial T}{\partial Y} = -1, \quad \frac{\partial C}{\partial Y} = -1 \quad \text{at } Y = 0, \end{aligned}$$

$$\begin{aligned} U = 0, \quad T = 0, \quad C = 0 \quad \text{at } X = 0, \\ U \rightarrow 0, \quad T \rightarrow 0, \quad C \rightarrow 0 \quad \text{as } Y \rightarrow \infty \end{aligned} \quad (14)$$

Knowing the velocity, temperature and concentration field it is customary to study the rate of shear stress, the rate of heat transfer and the rate of concentration. The dimensionless local as well as average values of the skin friction, the Nusselt number and the Sherwood number are given by the following expressions:

$$\tau_x = - \left\langle \frac{\partial U}{\partial Y} \right\rangle_{y=0} \quad (15)$$

$$\bar{\tau} = - \int_0^1 \left\langle \frac{\partial U}{\partial Y} \right\rangle_{Y=0} dX \quad (16)$$

$$Nu_x = -X \left\langle \frac{\partial T}{\partial Y} \right\rangle_{Y=0} \quad (17)$$

$$\overline{Nu} = - \int_0^1 \left\langle \frac{\partial T}{\partial Y} \right\rangle_{y=0} dX \quad (18)$$



$$Sh_X = X \left\langle \frac{\partial C}{\partial Y} \right\rangle_{y=0} \quad (19)$$

$$\overline{Sh} = - \int_0^1 \left\langle \frac{\partial C}{\partial Y} \right\rangle_{y=0} dX \quad (20)$$

## Numerical Technique:

In order to solve these unsteady, non-linear coupled equations (10) to (13) under the conditions (14), an implicit finite difference scheme of Crank-Nicolson type has been employed. The finite difference equations corresponding to equations (1) to (13) are as follows:

$$\frac{[U_{i,j}^{n+1} - U_{i-1,j}^{n+1} + U_{i,j}^n - U_{i-1,j}^n + U_{i,j-1}^{n+1} - U_{i-1,j-1}^{n+1} + U_{i,j-1}^n - U_{i-1,j-1}^n]}{4\Delta X} + \frac{[V_{i,j}^{n+1} - V_{i,j-1}^{n+1} + V_{i,j}^n - V_{i,j-1}^n]}{2\Delta Y} = 0. \quad (21)$$

$$\begin{aligned} & \frac{[U_{i,j}^{n+1} - U_{i,j}^n]}{\Delta t} + U_{i,j}^n \frac{[U_{i,j}^{n+1} - U_{i-1,j}^{n+1} + U_{i,j}^n - U_{i-1,j}^n]}{2\Delta X} + \\ & V_{i,j}^n \frac{[U_{i,j+1}^{n+1} - U_{i,j-1}^{n+1} + U_{i,j+1}^n - U_{i,j-1}^n]}{4\Delta Y} = \\ & Gr \frac{[T_{i,j}^{n+1} + T_{i,j}^n]}{2} + Gm \frac{[C_{i,j}^{n+1} + C_{i,j}^n]}{2} + \\ & \frac{[U_{i,j-1}^{n+1} - 2U_{i,j}^{n+1} + U_{i,j+1}^{n+1} + U_{i,j-1}^n - 2U_{i,j}^n + U_{i,j+1}^n]}{2(\Delta Y)^2}. \end{aligned} \quad (22)$$

$$\begin{aligned} & \frac{[T_{i,j}^{n+1} - T_{i,j}^n]}{\Delta t} + U_{i,j}^n \frac{[T_{i,j}^{n+1} - T_{i-1,j}^{n+1} + T_{i,j}^n - T_{i-1,j}^n]}{2\Delta X} + \\ & V_{i,j}^n \frac{[T_{i,j+1}^{n+1} - T_{i,j-1}^{n+1} + T_{i,j+1}^n - T_{i,j-1}^n]}{4\Delta Y} = \frac{1}{Pr} \left( 1 + \frac{4}{3N} \right) \\ & \frac{[T_{i,j-1}^{n+1} - 2T_{i,j}^{n+1} + T_{i,j+1}^{n+1} + T_{i,j-1}^n - 2T_{i,j}^n + T_{i,j+1}^n]}{2(\Delta Y)^2}. \end{aligned} \quad (23)$$

$$\begin{aligned}
& \frac{[C_{i,j}^{n+1} - C_{i,j}^n]}{\Delta t} + U_{i,j}^n \frac{[C_{i,j}^{n+1} - C_{i-1,j}^{n+1} + C_{i,j}^n - C_{i-1,j}^n]}{2\Delta X} + \\
& V_{i,j}^n \frac{[C_{i,j+1}^{n+1} - C_{i,j-1}^{n+1} + C_{i,j+1}^n - C_{i,j-1}^n]}{4\Delta Y} \\
& = \frac{1}{Sc} \frac{[C_{i,j-1}^{n+1} - 2C_{i,j}^{n+1} + C_{i,j+1}^{n+1} + C_{i,j-1}^n - 2C_{i,j}^n + C_{i,j+1}^n]}{2(\Delta Y)^2}. \quad (24)
\end{aligned}$$

The boundary condition at  $Y=0$  for the temperature in the finite difference form is

$$\frac{[T_{i,1}^{n+1} - T_{i-1,1}^{n+1} + T_{i,1}^n - T_{i-1,1}^n]}{4\Delta Y} = -1 \quad (25)$$

At  $Y=0$  (i.e.,  $j=0$ ), Eq (23) becomes

$$\begin{aligned}
& \frac{[T_{i,0}^{n+1} - T_{i,0}^n]}{\Delta t} + U_{i,0}^n \frac{[T_{i,0}^{n+1} - T_{i-1,0}^{n+1} + T_{i,0}^n - T_{i-1,0}^n]}{2\Delta X} + \\
& V_{i,0}^n \frac{[T_{i,1}^{n+1} - T_{i-1,1}^{n+1} + T_{i,1}^n - T_{i-1,1}^n]}{4\Delta Y} = \quad (26)
\end{aligned}$$

$$\frac{1}{Pr} \left( 1 + \frac{4}{3N} \right) \frac{[T_{i-1,1}^{n+1} - 2T_{i,0}^{n+1} + T_{i,1}^{n+1} + T_{i-1,1}^n - 2T_{i,0}^n + T_{i,1}^n]}{2(\Delta Y)^2}.$$

After eliminating  $T_{i,1}^{n+1} + T_{i-1,1}^{n+1}$  using Eq. (25), Eq. (26) reduces to the form

$$\begin{aligned}
& \frac{[T_{i,0}^{n+1} - T_{i,0}^n]}{\Delta t} + U_{i,0}^n \frac{[T_{i,0}^{n+1} - T_{i-1,0}^{n+1} - T_{i,0}^n + T_{i-1,0}^n]}{2\Delta X} = \\
& \frac{1}{Pr} \left( 1 + \frac{4}{3N} \right) \frac{[T_{i,1}^{n+1} - T_{i,0}^{n+1} + T_{i,1}^n - T_{i,0}^n + 2\Delta Y]}{2(\Delta Y)^2}. \quad (27)
\end{aligned}$$

The boundary condition at  $Y=0$  for the concentration in the finite difference form is

$$\frac{[C_{i,1}^{n+1} - C_{i-1,1}^{n+1} + C_{i,1}^n - C_{i-1,1}^n]}{4\Delta Y} = -1 \quad (28)$$

At  $Y=0$ (i.e.,  $j=0$ ), Eq. (24) becomes

$$\begin{aligned} & \frac{[C_{i,0}^{n+1} - C_{i,0}^n]}{\Delta t} + U_{i,0}^n \frac{[C_{i,0}^{n+1} - C_{i-1,0}^{n+1} + C_{i,0}^n - C_{i-1,0}^n]}{2\Delta X} + \\ & V_{i,0}^n \frac{[C_{i,1}^{n+1} - C_{i-1,1}^{n+1} + C_{i,1}^n - C_{i-1,1}^n]}{4\Delta Y} = \\ & \frac{1}{Pr} \left(1 + \frac{4}{3N}\right) \frac{[C_{i-1}^{n+1} - 2C_{i,0}^{n+1} + C_{i,1}^{n+1} + C_{i-1}^n - 2C_{i,0}^n + C_{i,1}^n]}{(\Delta Y)^2}. \end{aligned} \quad (29)$$

After eliminating  $C_{i,1}^{n+1} + C_{i-1,1}^{n+1}$  using Eq (28), Eq (29) reduces to the form

$$\begin{aligned} & \frac{[C_{i,0}^{n+1} - C_{i,0}^n]}{\Delta t} + U_{i,0}^n \frac{[C_{i,0}^{n+1} - C_{i-1,0}^{n+1} + C_{i,0}^n - C_{i-1,0}^n]}{2\Delta X} = \\ & \frac{1}{Sc} \frac{[C_{i,1}^{n+1} - C_{i,0}^{n+1} + C_{i,1}^n - C_{i,0}^n + 2\Delta Y]}{(\Delta Y)^2}. \end{aligned} \quad (30)$$

The region of integration is considered as a rectangle with sides  $X_{max}(= 1)$  and  $Y_{max}(= 14)$  corresponds to  $Y = \infty$ , which lies very well outside the momentum, energy and concentration boundary layers. The maximum of  $Y$  was chosen as 14 after some preliminary investigations so that the last two of the boundary conditions of Eq. (14) are satisfied. Here, the subscript  $i$ -designates the grid point along the  $X$ -direction,  $j$ -along the  $Y$ -direction and the superscript  $n$  along the  $t$ -direction. An appropriate mesh sizes considered for the calculation is  $\Delta X = 0.05$ ,  $\Delta Y = 0.25$ , and the time step  $\Delta t = 0.01$ . During any one time step, the coefficients  $U_{i,j}^{n+1}$  and  $V_{i,j}^{n+1}$  appearing in the difference equations are treated as constants. The values of  $C, T, U$  and  $V$  at time level  $(n + 1)$  using the known values at previous time level  $(n)$  are calculated as follows. The finite difference Eqs. (30) and (28) at every internal nodal point on a particular  $i$ -level constitute a tridiagonal system of equations. Such a system of equations are solved by using Thomas algorithm as discussed in Carnahan et al. [22]. Thus, the values of  $C$  are known at every internal nodal point on a particular  $i$  at  $(n + 1)$ -th time level. Similarly, the values of  $T$  are calculated from Eqs. (27) and (25). Using the values of  $C$  and  $T$  at  $(n + 1)$ -th time level in Eq. (22), the values of  $U$  at  $(n + 1)$ -th time level are found in similar manner. Then the values

of  $V$  are calculated explicitly using the Eq. (21) at every nodal point at particular  $i$ -level at  $(n+1)$ th time level. This process is repeated for various  $i$ -levels. Thus the values of  $C, T, U$  and  $V$  are known, at all grid points in the rectangular region at  $(n + 1)$ th time level. Computations are carried out until the steady-state is reached. The steady-state solution is assumed to have been reached, when the absolute difference between the values of  $U$  as well as temperature  $T$  and concentration  $C$  at two consecutive time steps are less than  $10^{-5}$  at all grid points.

After experimenting with few sets of mesh, they have been fixed at the level  $\Delta X = 0.05, \Delta Y = 0.25$ , and the time step  $\Delta t = 0.01$ . In this case, spatial mesh sizes are reduced by 50% in one direction, and then in both directions, and the results are compared. It is observed that, when mesh size is reduced by 50% in X-direction or both X and Y directions, the results are correct to fourth decimal places. The computer takes more time to compute, if the size of the time-step is small. Hence, the above-mentioned sizes have been considered as appropriate mesh sizes have been considered as appropriate mesh sizes for calculations.

## Results and Discussion

In order to check the accuracy of our numerical results, the present study is compared with the available theoretical solution of Soundalgekar and Patil [5], and they are found to be in good agreement.

The transient velocity, temperature and concentration profiles are different physical parameters such as  $Gr, Gm, Sc, M, N$  and  $Pr$  are shown in Figs.1.to 9 at  $X = 1.0$ . In Fig.2 the steady state velocity profiles are presented for different values of buoyancy force parameter  $Gr$  or  $Gm$  and  $N$ . The time required to reach the steady state for smaller values of  $Gr = Gm(= 2)$  is 8.70,9.45,9.75 respectively, where as for large  $Gr = Gm(= 4)$  the steady state for smaller vales of  $Gr = Gm(= 2)$  the steady state is reached at 7.75,8.58,8.79 respectively, which leads to conclude that increased in buoyancy force parameter reduces the time taken to reach the steady state. It can also be seen that increase in radiation parameter  $N$  leads to a decrease in velocity profiles.

In Fig.3, steady state velocity profiles for different values of  $Gr$  or  $Gm, Sc, N$  and for fluid Prandtl number,  $Pr = 0.71$  are shown. From

Fig.3 it can be concluded that velocity decreases due to an increase in the Schmidt number  $Sc$ . In these Figs.2 and 3, for  $Sc = 2.0$  is larger than  $Pr = 0.71$  and hence concentration layer is thinner than thermal layer. This confirms the downward flow to a thin region near the surface. For lower  $Sc$  the thickness of the concentration layer increases and the region of flow extend farther away from the plate. Figs. 4 and 5 illustrate the influence of the magnetic parameter  $M$  on the velocity and temperature profiles in the boundary layer respectively. Application of a transverse magnetic field to an electrically conducting gives rise to a resistive type of force called Lorenz force. This force has the tendency to slowdown the motion of the fluid in the boundary layer and to increase its temperature also, the effects on the flow and thermal fields become more so as the strength of the magnetic field increases. This is obvious from the decrease in the velocity and the increase in the temperature profiles presented in 4 and 5. Fig 6 shows that the temperature decreases with the increasing values of  $Gr$  or  $Gm$ .

In Fig.7, it is seen that the time required to reach the steady state is more at higher values of  $N = 10$  as compared to the lower values of  $N = 5$ . It is also observed that the temperature increases with the increasing Schmidt number.

From Figs.1 to 7 it is observed that owing to an increase in the value of the radiation parameter  $N$ , both momentum and thermal boundary layer thickness decrease. However the time taken to reach the steady state increases as  $N$  increases. At small values of  $N$ , the velocity and temperature of the fluid increases sharply near the plate as the time  $t$  increases, which totally absent in the absence of radiation effects.

From Fig.8, the effect of buoyancy force parameter  $Gr$  or  $Gm$  on time taken to reach the steady state conditions are shown graphically. For  $Gr = Gm (= 2)$  the time required to reach the steady state when  $N = 3, 5, 10$  are 8.70, 9.54 and 9.75 respectively where as for large  $Gr = Gm (= 4)$  the time required to reach the steady state are 7.75, 8.58 and 8.79 respectively. Which leads to conclude that when the buoyancy force parameter  $Gr$  or  $Gm$  increases, the time required to reach the steady state is reduced. Transient concentration profiles for  $Pr = 0.71, Gr = Gm (= 2), N = 5, 10$  and  $Sc = 0.78$  and 2.0 are shown Fig.9. it is observed that for small values of  $Sc = 0.78$  and  $N = 5$  the time taken to reach the steady state is 9.64 where as when  $N = 10$ , under similar conditions, the time required to reach the

state is 9.82 from which it is concluded that for higher value of  $N$ , the time taken to reach the steady state is more when  $Sc$  is small. In Fig.10, steady state concentration profiles are plotted for different values of Schmidt number and magnetic field parameter  $M$ . As expected concentration is lower for systems with a larger  $Sc$ . Concentration increases with increase in  $M$ .

Steady state local skin-friction  $\tau_X$  profiles are plotted in Fig.11 against the axial coordinate  $X$ . The local shear stress  $\tau_X$  increases with the increasing value of  $Sc$  and decreasing value of  $Gr$  and  $Gm$ . The average values of skin friction  $\bar{\tau}$  for different  $Gr, Gm, Sc$  and  $N$  are shown in Fig.12. It is noted that  $\bar{\tau}$  decreases with decreasing values of  $Sc$ , but increases with decreasing values of  $Gr$  or  $Gm$  throughout the transient period and at the steady state level. It is also observed that the average skin-friction  $\bar{\tau}$  increases as the radiation interaction parameter  $N$  increases. The local Nusslet number  $Nu_X$  for different  $Gr, Gm, Sc$  and  $N$  are shown in Fig.13. Local heat transfer rate  $Nu_X$  decreases with increasing values of  $Sc$  and increases with increasing  $Gr$  or  $Gm$ . For increasing values of radiation parameter  $N$ , the local Nusselt number  $Nu_X$  increases. The trend is just opposite in case of local Sherwood number  $Sh_X$  with respect to  $Gr, Gm, Sc$  and  $N$  (Fig.15). From Fig.14 it is observed that the average Nusselt number  $\overline{Nu}$  increases with increasing values of  $Gr$  or  $Gm$  and  $N$ . From Fig.16, we can easily see that the average Sherwood number  $\overline{Sh}$  increases as  $Gr$  or  $Gm$  and  $Sc$  increases.

## Conclusions

A detailed numerical study has been carried out for the radiative MHD flow past an impulsively started vertical plate with uniform heat and mass flux. The dimensionless governing equations are solved by an implicit finite-difference method of Crank-Nicolson type. Conclusions of the study are as follows.

1. The magnetic field parameter has retarding effect on the velocity.
2. Temperature and concentration increases with increasing value of the magnetic field parameter.
3. In case of  $Sc$ , the velocity and concentration profiles are decreasing as  $Sc$  increases.

4. The time required to reach the steady state increases as radiation parameter increases.
5. At small values of the radiation parameter, the velocity and temperature of the fluid increases sharply near the late as the time  $t$  increase, which is totally absent in the absence of radiation effects.
6. The local and average skin-friction decreases with increasing  $Gr$  or  $Gm$  and increases with increasing value of  $N$  and  $Sc$ . The local and average Nusselt number increases with the increasing value of radiation parameter. The average Sherwood number increases as  $Gr$  or  $Gm$  and  $Sc$  increases.

## References

- [1] Stokes, G.G., On the effect of internal friction of fluids on the motion of pendulums. Cambridge Phil.Trans, IX, 8-106(1851).
- [2] Stewartson.K, On the impulsive motion of a flat plate in a viscous plate. Quarterly Journal of Mechanics and Applied Mathematics, 4(1951) 182-198.
- [3] Hall, M.G. Boundary layer over an impulsively started flat plate. Proc. Royal Soc. London 310A: 401-414.
- [4] Soundalgekar, V.M., Free convection effects on the Stokes problem for an infinite vertical plate. Trans on ASME Journal of Heat Transfer 99(1977) 499-501.
- [5] Soundalgekar, V.M., Patil, M.R., Stokes problem for a vertical plate with constant heat flux, Astrophys.Space Sci.70(1980) 179-182.
- [6] Muthucumaraswamy, R, Ganesan.P., First-order chemical reaction on flow past an impulsively started vertical plate with uniform heat and mass flux. Acta Mech 147 (2001) 45-57.
- [7] Soundalgekar, V.M., Effects of mass transfer and free convection currents on the flow past an impulsively started vertical plate. Journal of Appl.Mech 46(1979) 757-760.

- [8] Soundalgekar, V.M., Gupta, S.K., Birajdar, N.S., Effects of mass transfer and free effects on MHD Stokes problem for a vertical plate, Nucl.Eng.Des.53 (1979)309-346.
- [9] Elbashbeshy, E.M.A, Heat and mass transfer along a vertical plate surface tension and concentration in the presence of magnetic field,Int.J.Eng.Sci,34(5) (1997)515-522.
- [10] Helmy, K.A, MHD unsteady free convection flow past a vertical porous plate. ZAMM 78(1998) 255-270.
- [11] Cess, R.D, The interaction of thermal radiation with free convection heat transfer. Int.J.Heat Mass Transfer. 9 (1966) 1269-1277.
- [12] Vedat S.Arpaçi: Effect of thermal radiation on the laminar free convection from a heated vertical plate. Int.J.Heat Mass Transfer, 11(1968), 871-881.
- [13] Cheng, E.H, Ozisik, M.N, Radiation with free convection in an absorbing, emitting and scattering medium. Int.J.Heat Mass Transfer, 15(1972) 1243-1252.
- [14] Raptis, A., Radiation and free convection flow through a porous medium.Int.Comm.Heat Mass Transfer 25 (2) (1998) 289-295.
- [15] Hossain, M.A., Takhar, H.S., Radiation effects on mixed convection along a vertical plate with uniform surface temperature, Heat Mass Transfer 31(1996)243-248.
- [16] M.H. Mansour, Radiative and free convection effects on the oscillatory flow past a vertical plate, Astrophysics and space science 166(1990),26-75.
- [17] Raptis, A, C.Perdikis, Radiation and free convection flow past a moving plate, Appl.Mech.Eng.4 (1999), 817-821.
- [18] Das, U.N, R.Deka, V.M.Soundalgekar, Radiation effects on flow past an impulsively started vertical plate-an exact solution, J.Theo.Appl.Fluid Mech,1(2)(1996)111-115.
- [19] Chamkha, A.J. Takhar, H.S. and Soundalgekar, V.M., Radiation effects on free convection flow past a semi-infinite vertical plate with mass transfer. Chem.Engg.J 84,335-342 (2001).



- [20] Ganesan, P and Loganathan, P. Radiation and mass transfer effects on flow of an incompressible viscous fluid past a moving cylinder. *Int.J.Heat. Mass Transfer* 45, 4281-4288 (2002).
- [21] Brewster, M.Q. *Thermal radiative transfer and properties*. John Wiley & sons. Inc., New York, 1992.
- [22] Carnahan, B., Luther, H.A., Wilkes, J.O.: *Applied numerical methods*, John Wiley and sons, New York, 1969.

Submitted on July 2005.

## **Prelazno radijaciono hidromagnetsko slobodno konvektivno tečenje preko impulsno pokrenute vertikalne ploče sa uniformnim toplotnim i masenim fluksom**

UDK 536.7, 536.84

Analizira se interakcija slobodne konvekcije sa termičkom radijacijom viskozno nestišljivog nestacionarnog MHD-tečenja sa uniformnim toplotnim i masenim fluksom. Ovaj tip problema se javlja pri primeni mnogih tehničkih oblasti kao: raketnih sistema, aerotermodinamike, aerodinamike kosmičkog leta, fizike plazme, proizvodnje stakla i tehnike grejača. Rosseland-ova aproksimacija se ovde koristi za opis radijacionog prenosa toplote u graničnom slučaju optički tankog fluida. Nelinearne spregnute jednačine se rešavaju implicitnom metodom konačnih razlika Crank-Nicolson-ovog tipa. Brzina, temperatura i koncentracija tečenja su prikazane za razne vrednosti parametara kao: termički Grashof-ov broj, maseni Grashof-ov broj, Prnadt-ov broj, Schmidt-ov broj, radijacioni parametar i magnetski parametar. Lokalno i prosečno skin-trenje, Nusselt-ov broj i Sherwood-ov broj su takodje grafički prikazani. Primećeno je da sa porastom radijacionog parametra raste brzina dok temperatura opada u graničnom sloju.

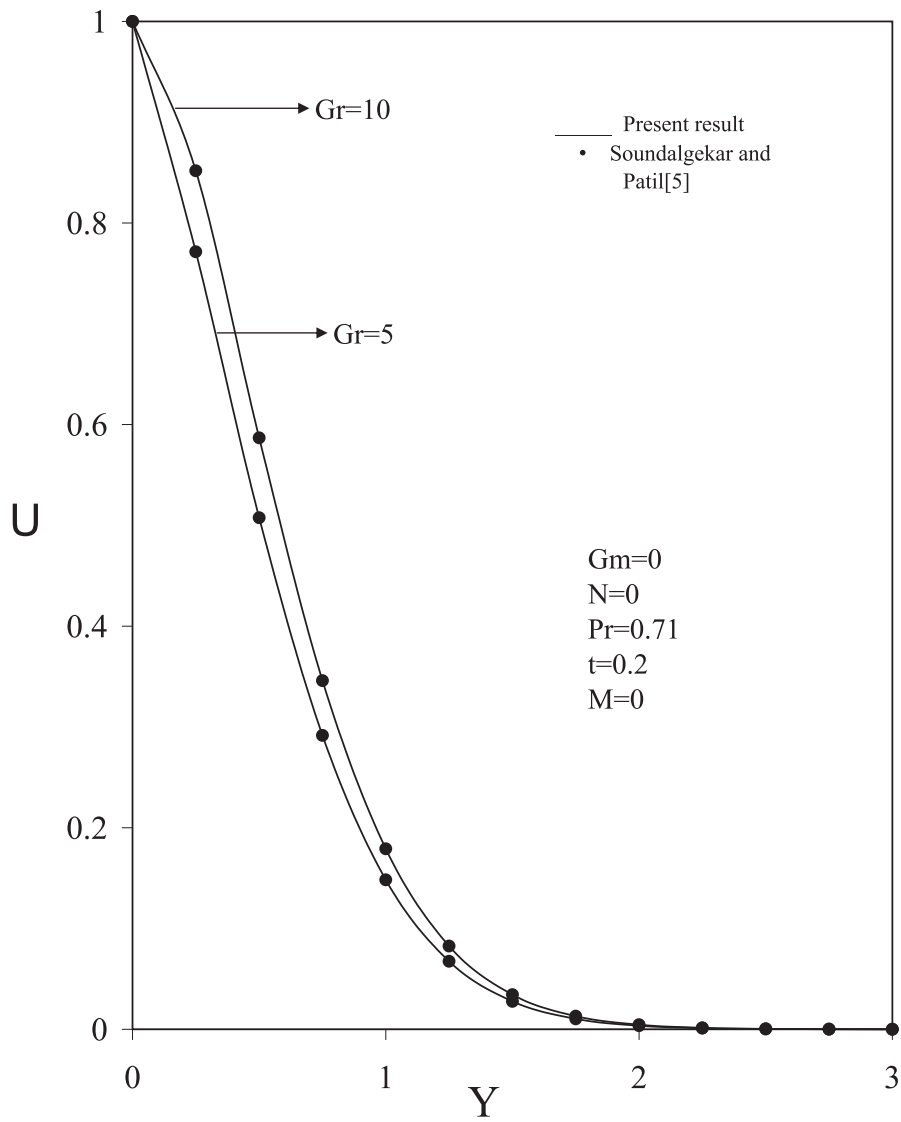


Figure 1: Comparison of velocity profiles.

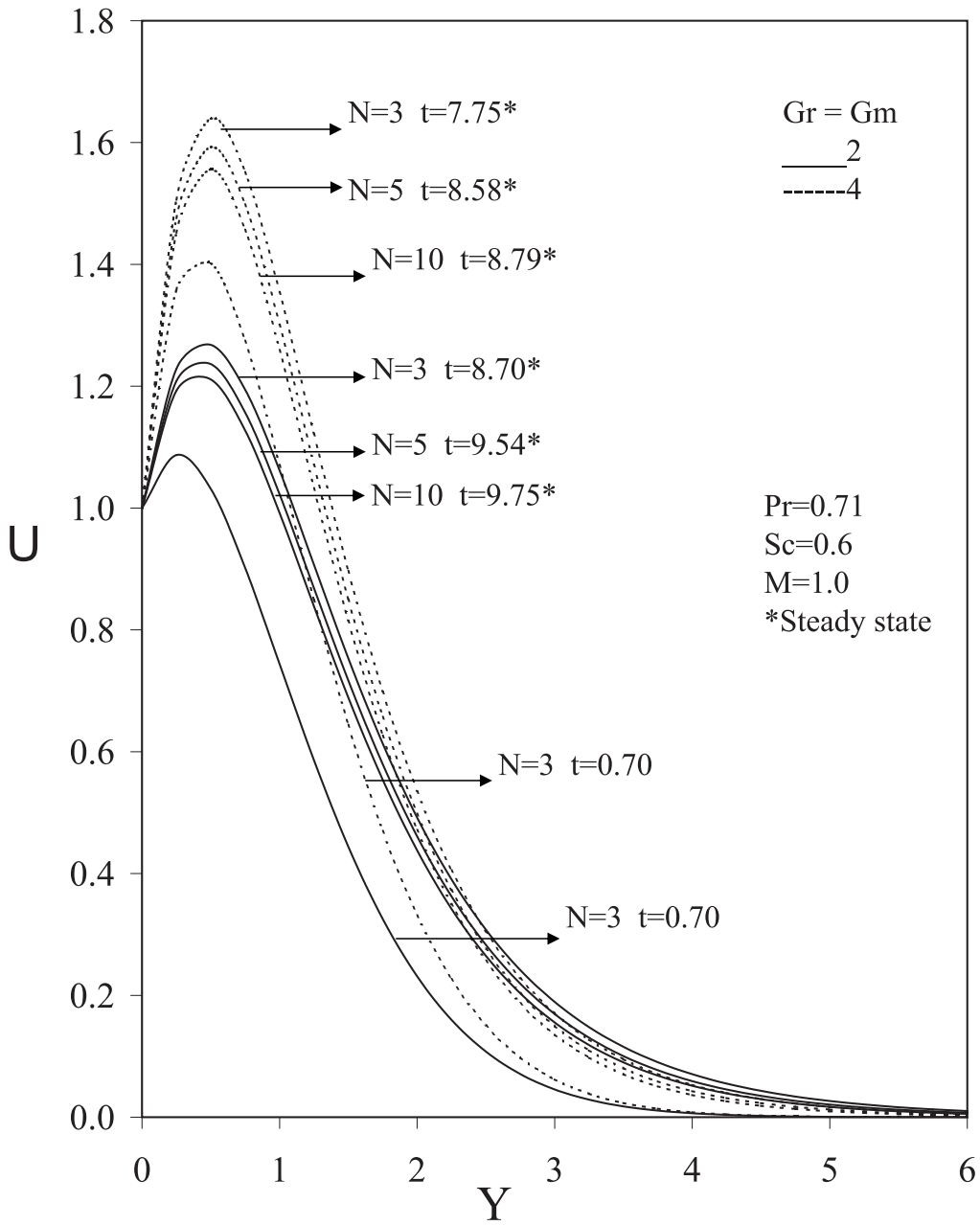


Figure 2: Transient velocity profiles at  $X = 1.0$  for different  $Gr, Gm, N$ .

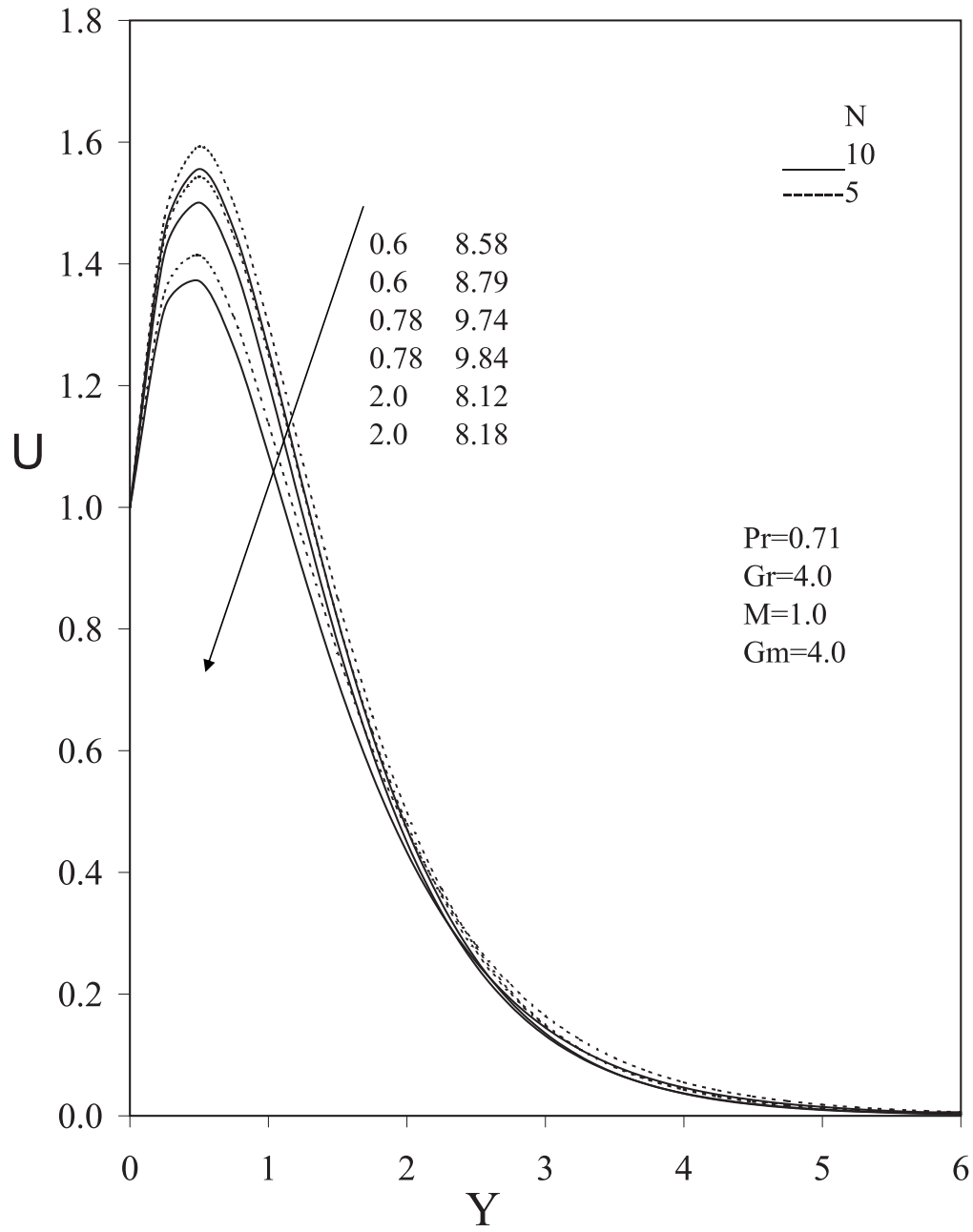


Figure 3: Steady state velocity profiles at  $X = 1.0$  for different  $Sc$ .

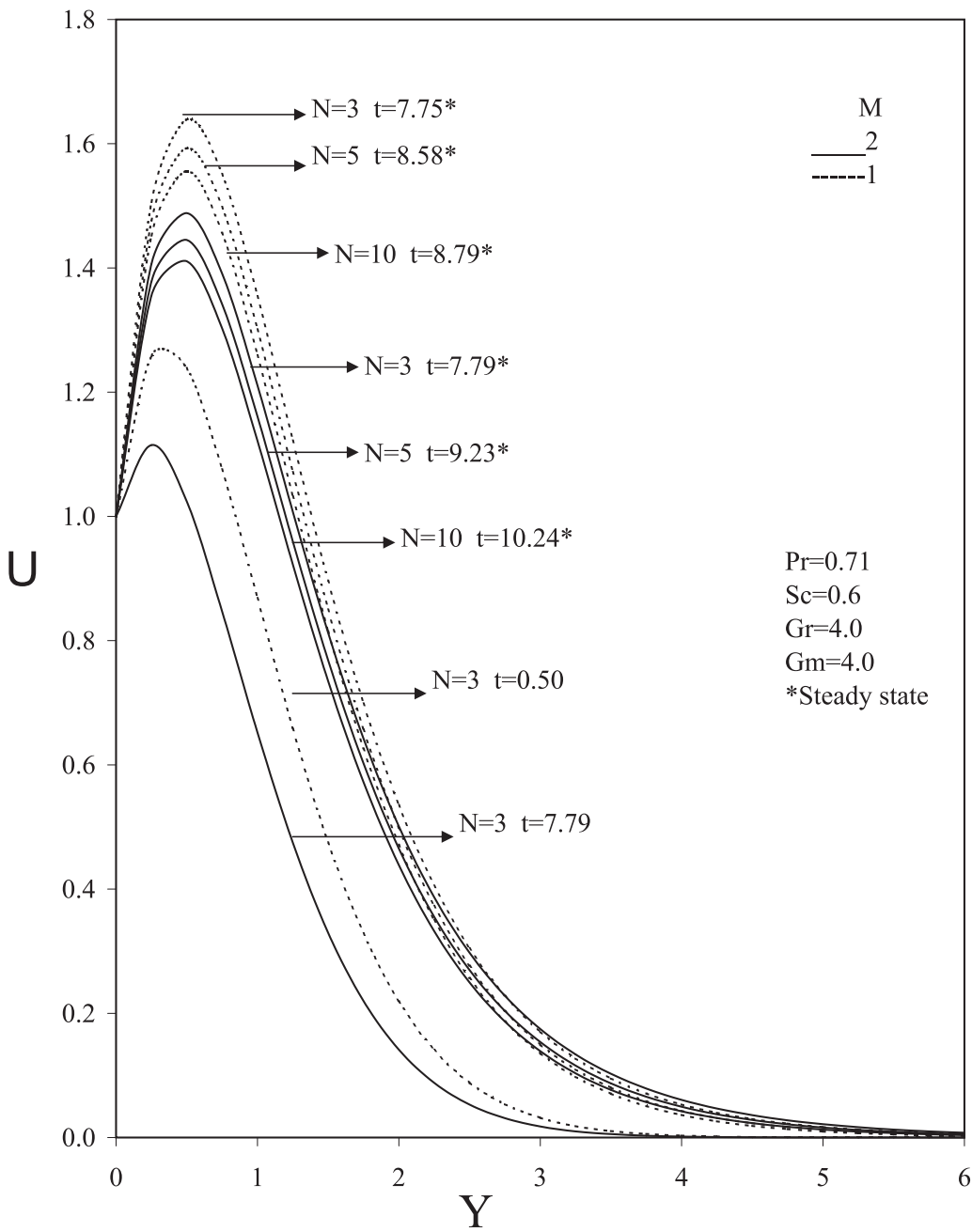


Figure 4: Transient velocity profiles for different  $N$  and  $M$

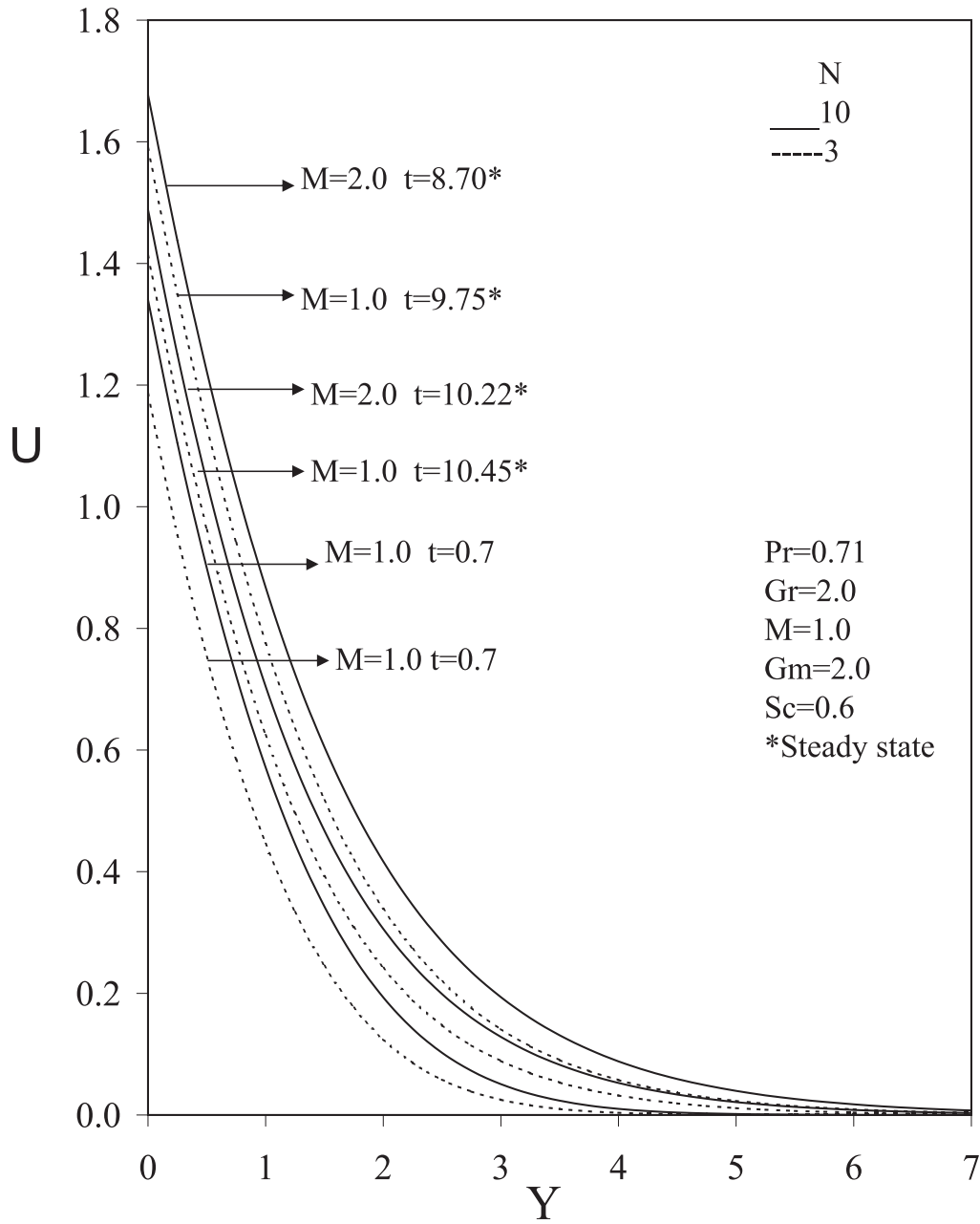


Figure 5: Transient temperature profiles for different  $N$  and  $M$

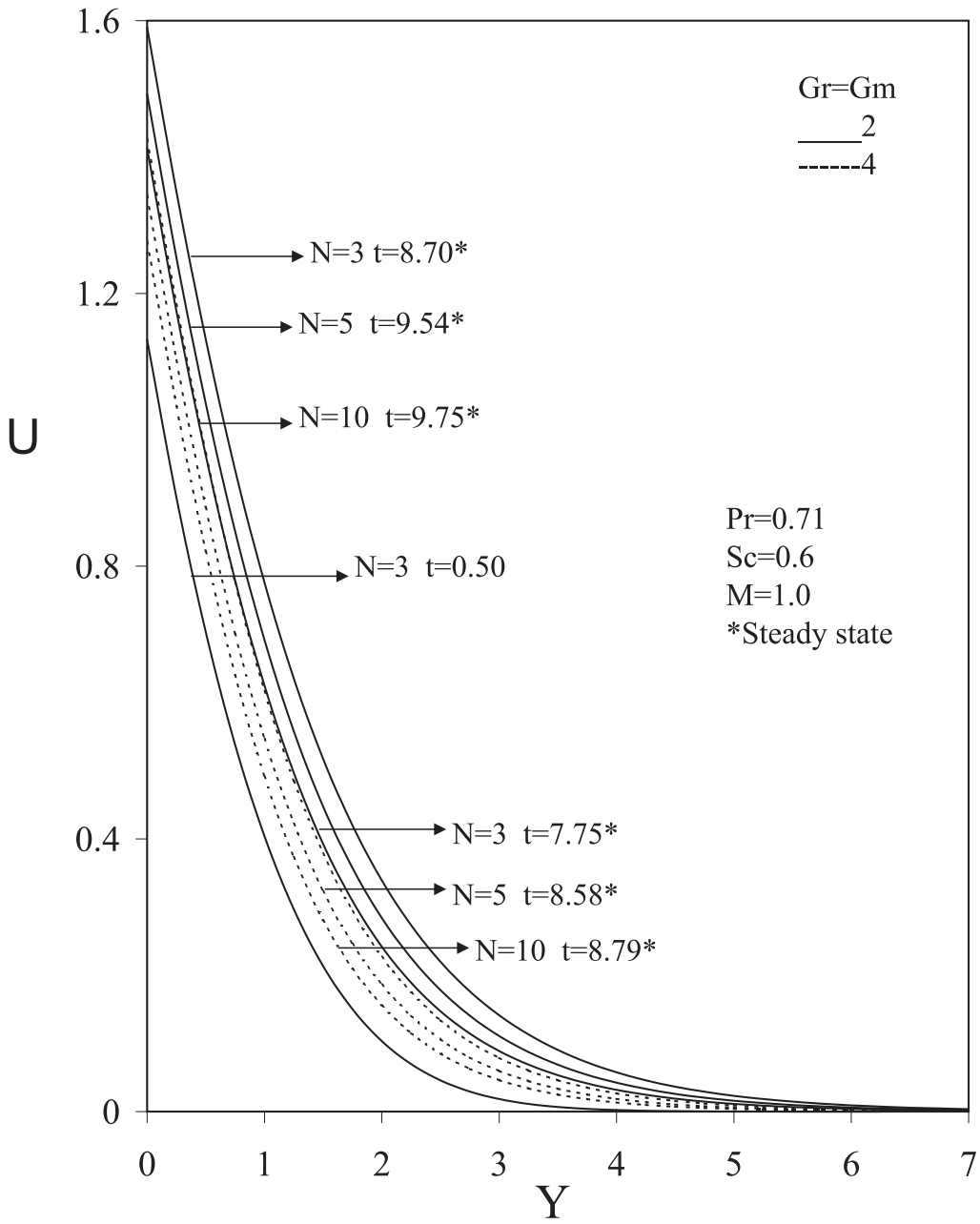


Figure 6: Transient temperature profiles at  $X = 1.0$  for different  $Gr, Gm, N$ .

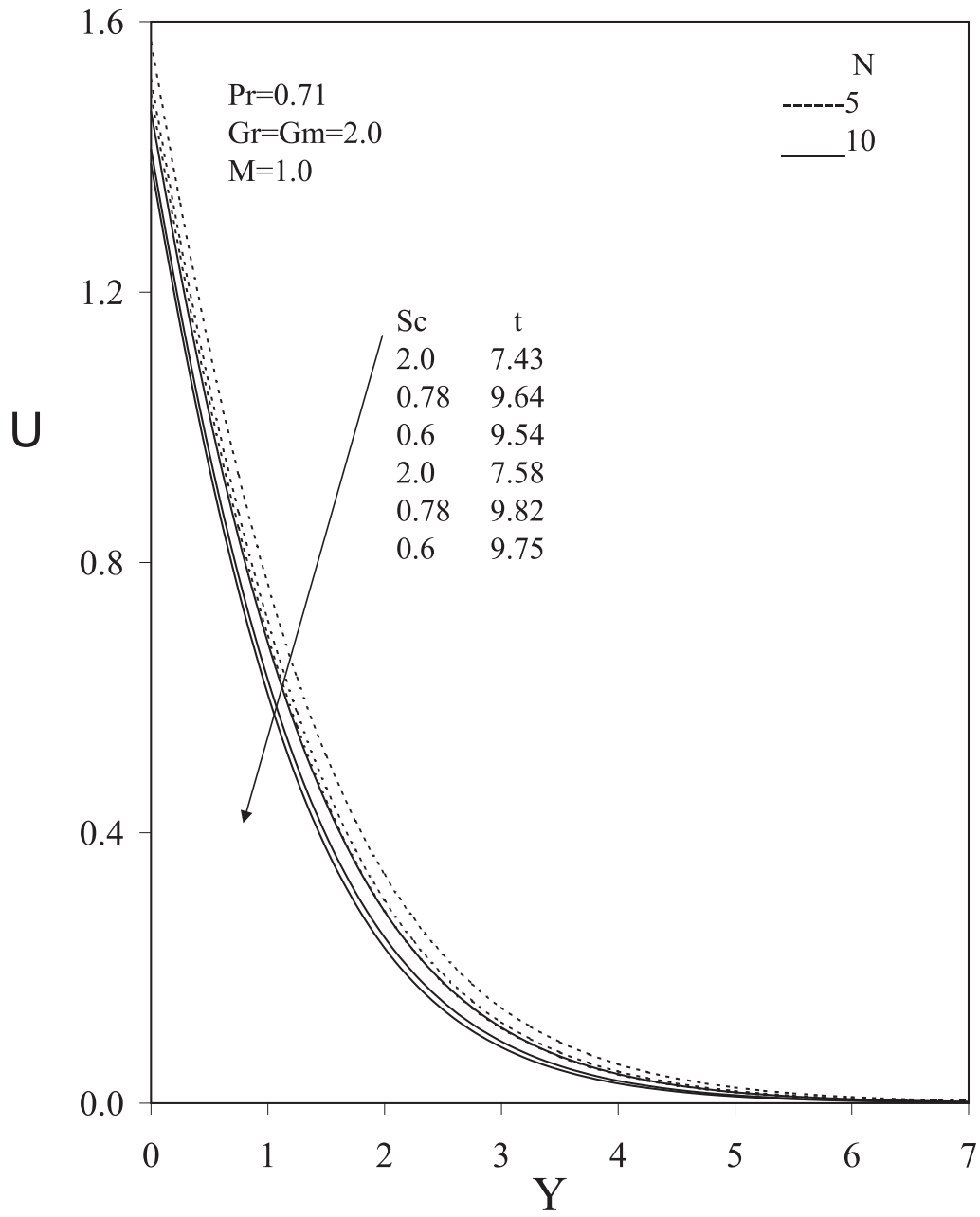


Figure 7: Transient temperature profiles for different  $N$  and  $Sc$ .



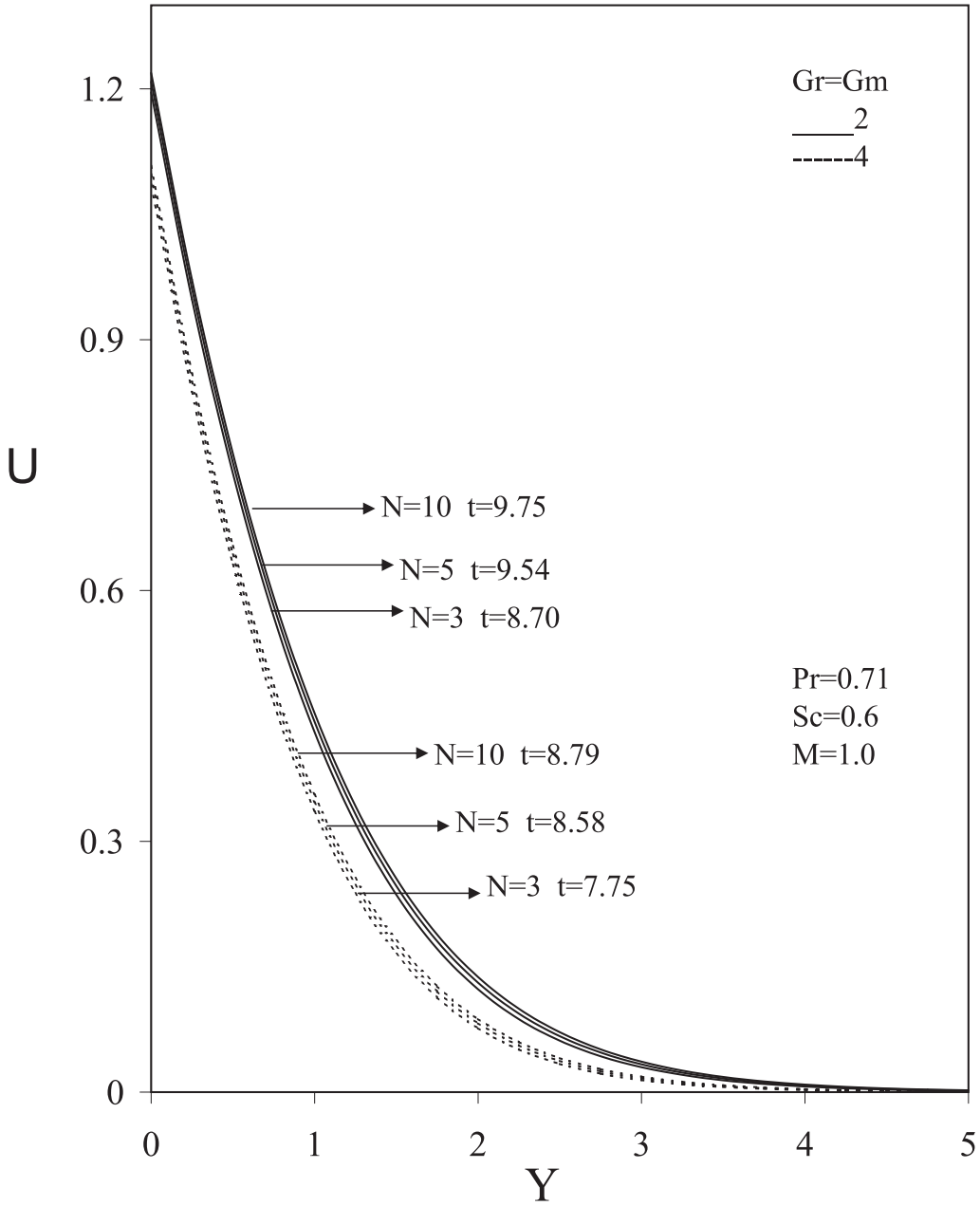


Figure 8: Steady state concentration profiles at  $X = 1.0$  for different  $Gr, Gm, N$ .

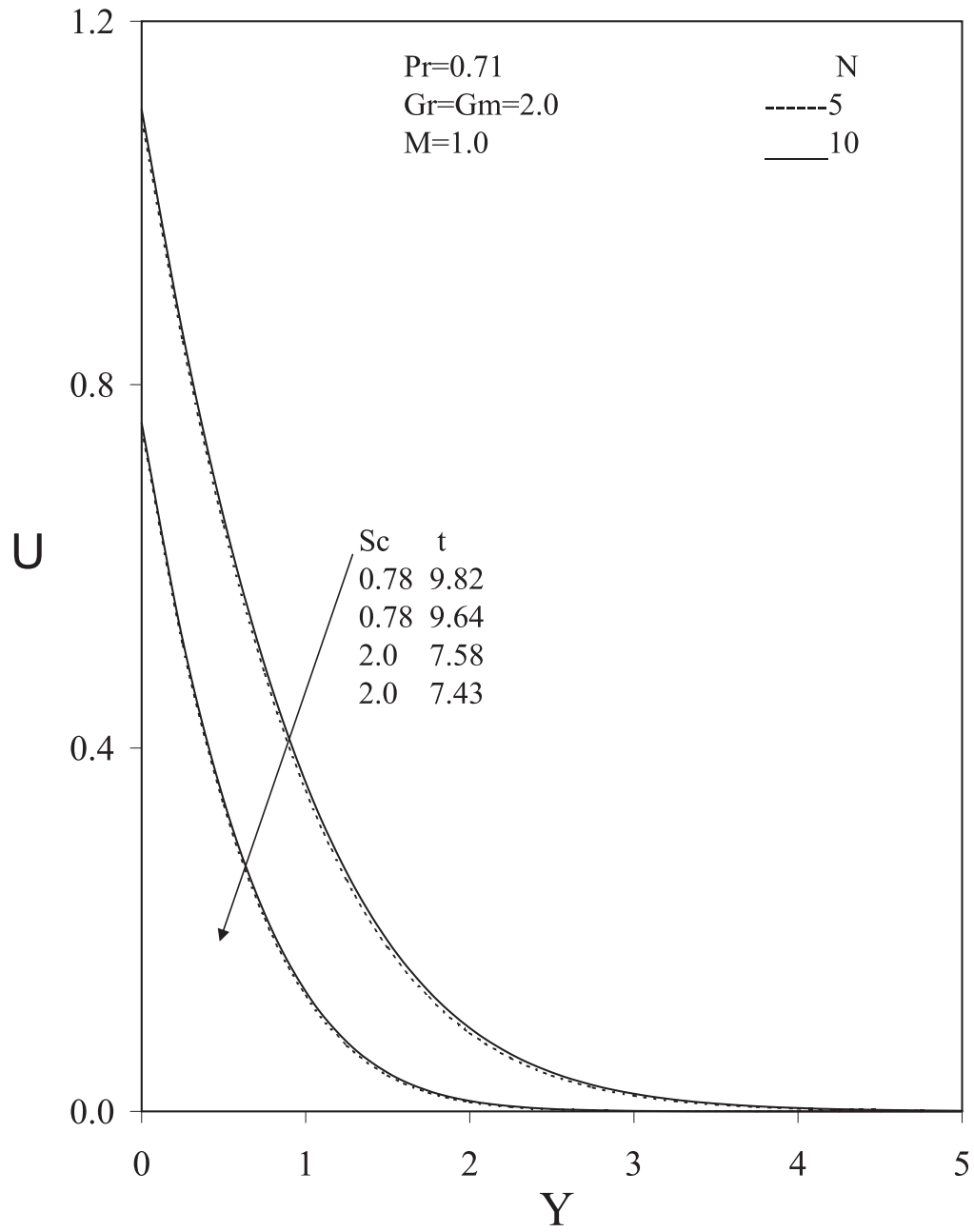


Figure 9: Steady state concentration profiles at  $X = 1.0$  for different  $Gr, Gm, N$ .

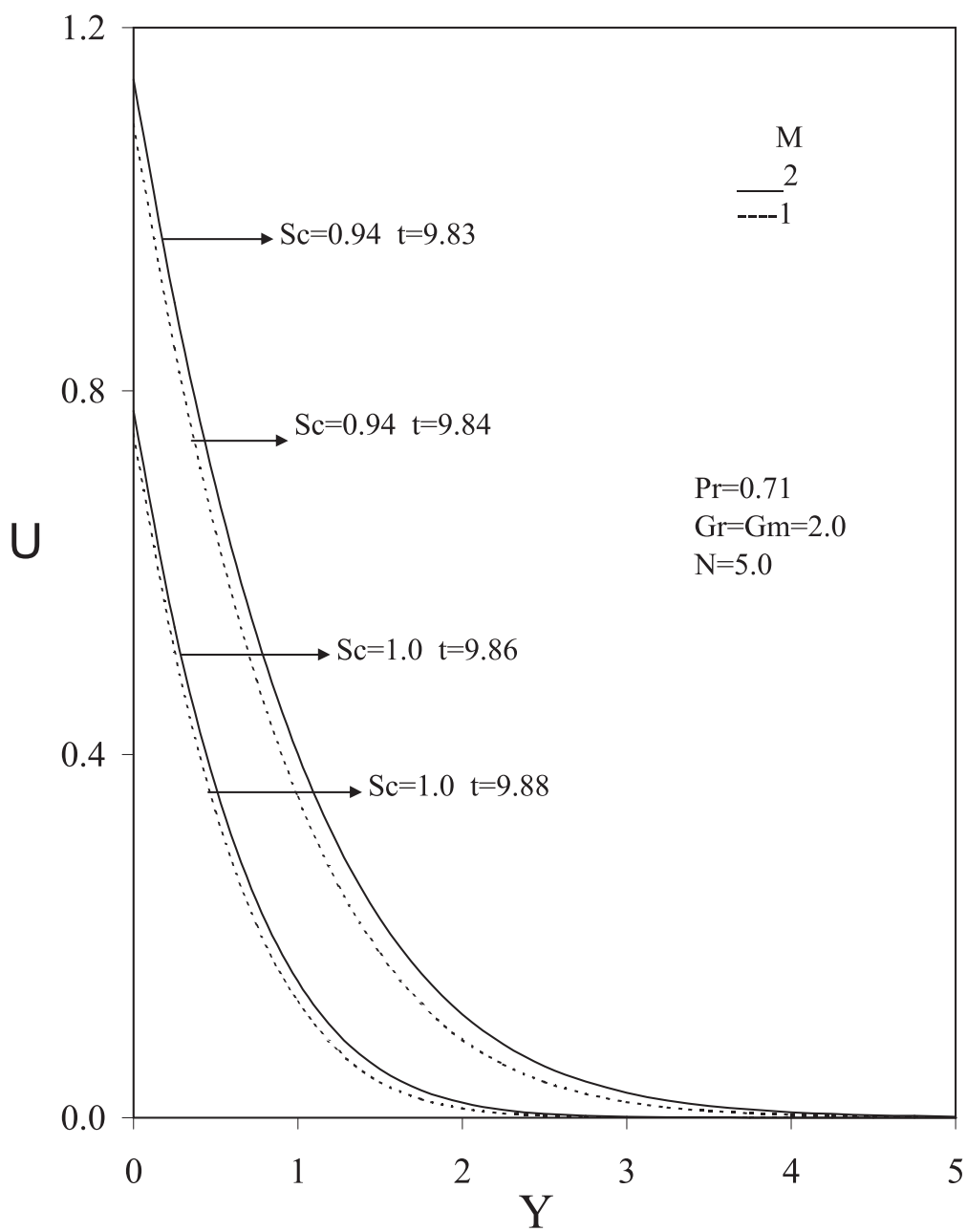


Figure 10: Steady state concentration profiles for different  $Sc$  and  $M$ .

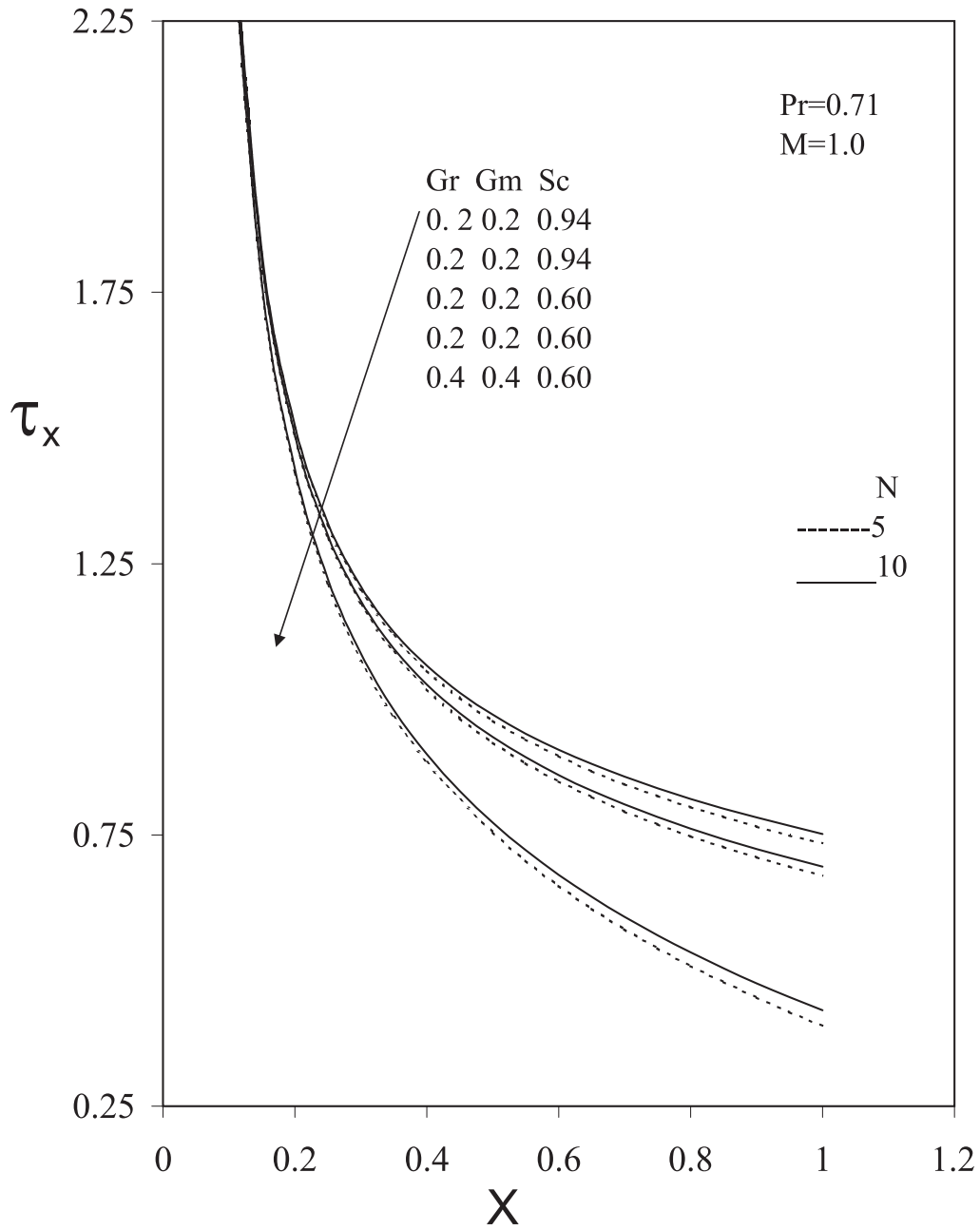


Figure 11: Local skin friction.

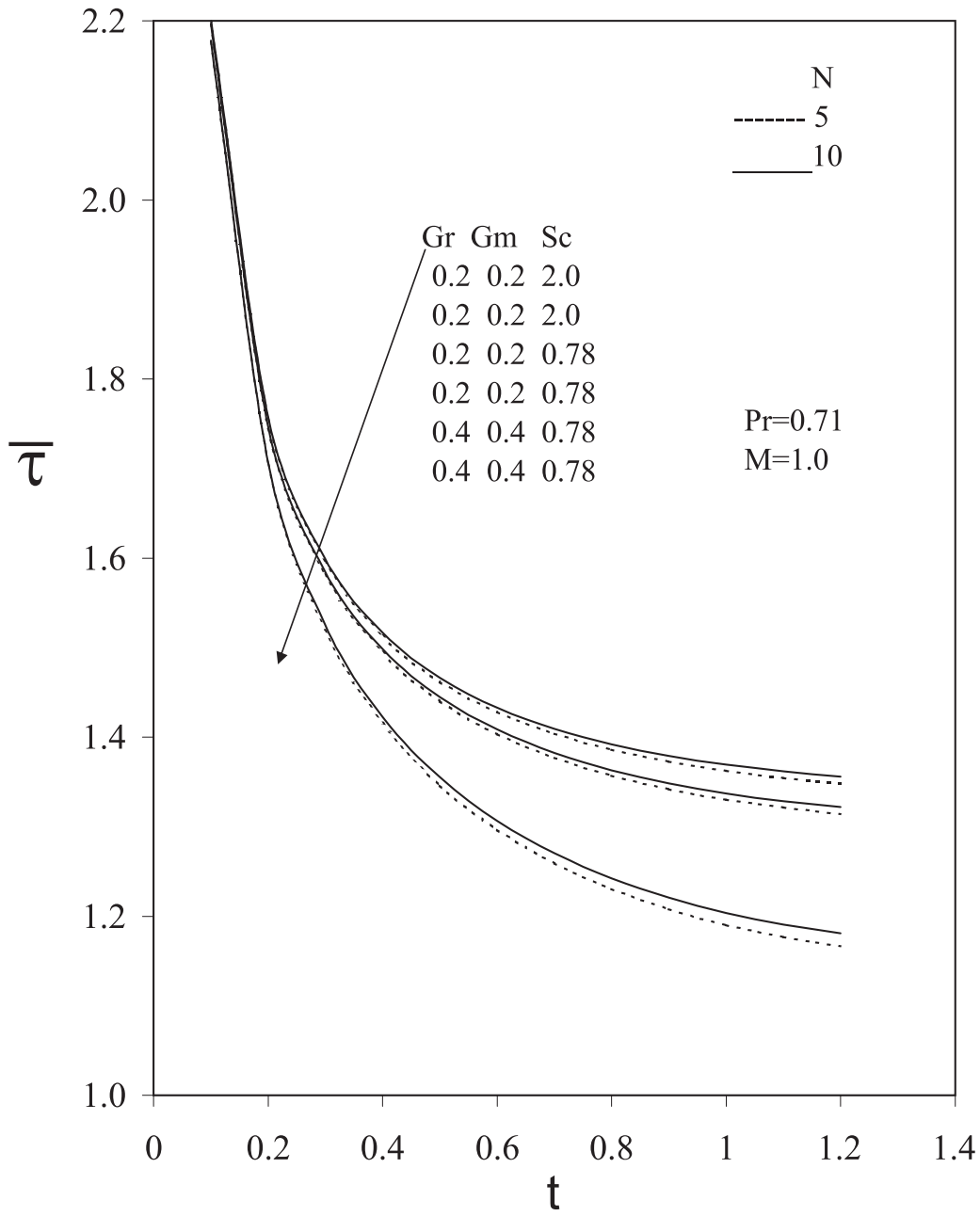


Figure 12: Average skin friction.

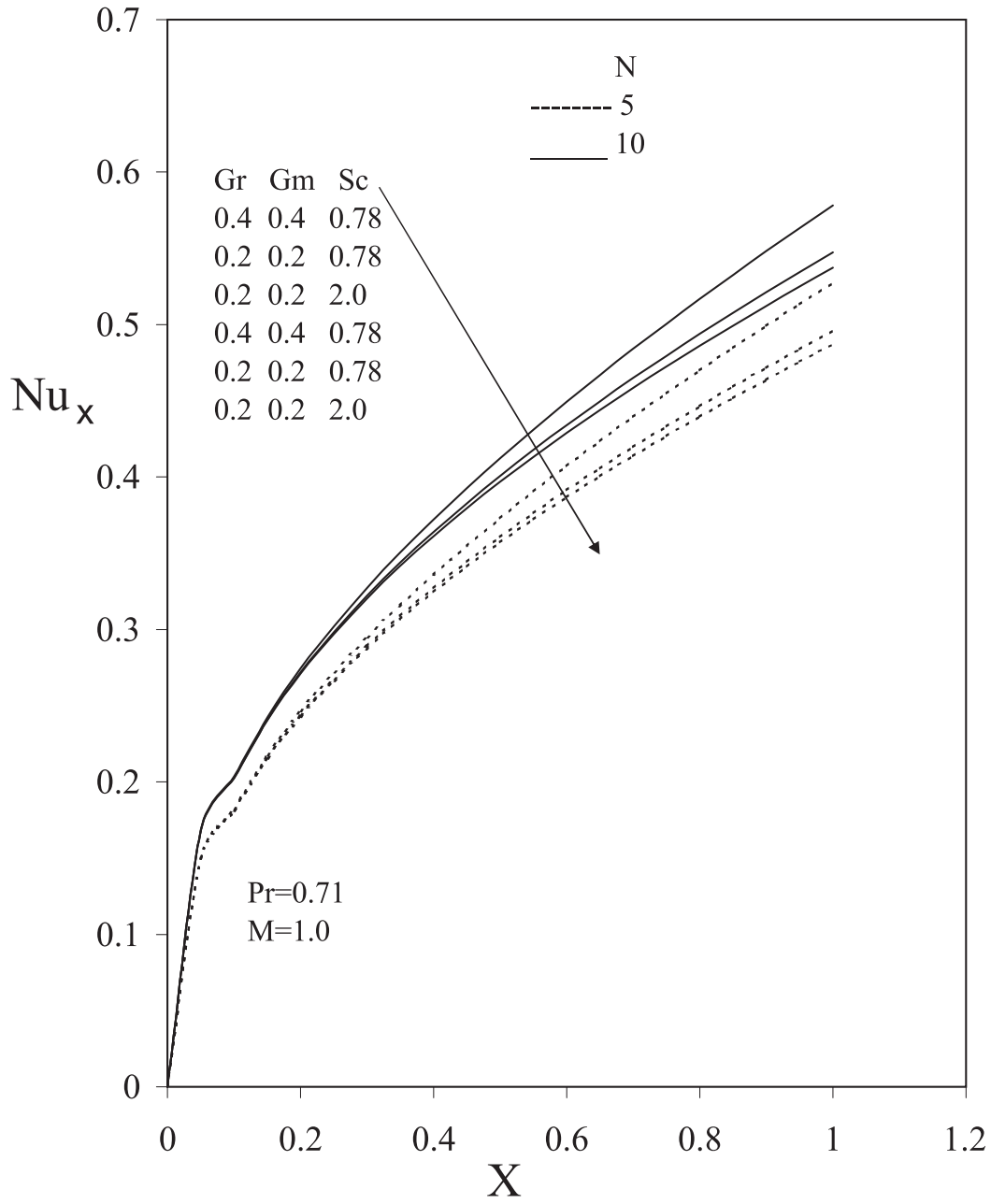


Figure 13: Local Nusselt number.

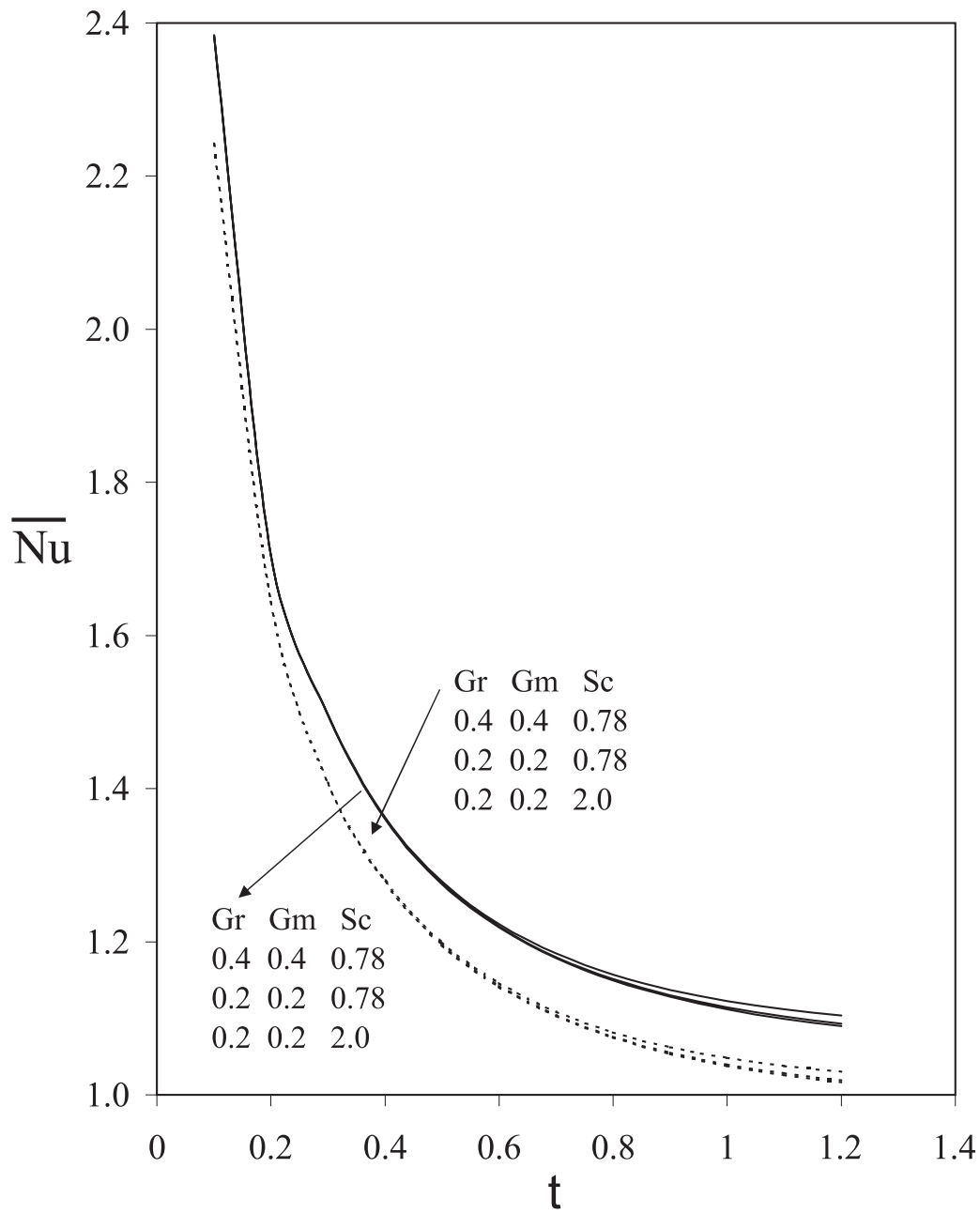


Figure 14: Average Nusselt number.

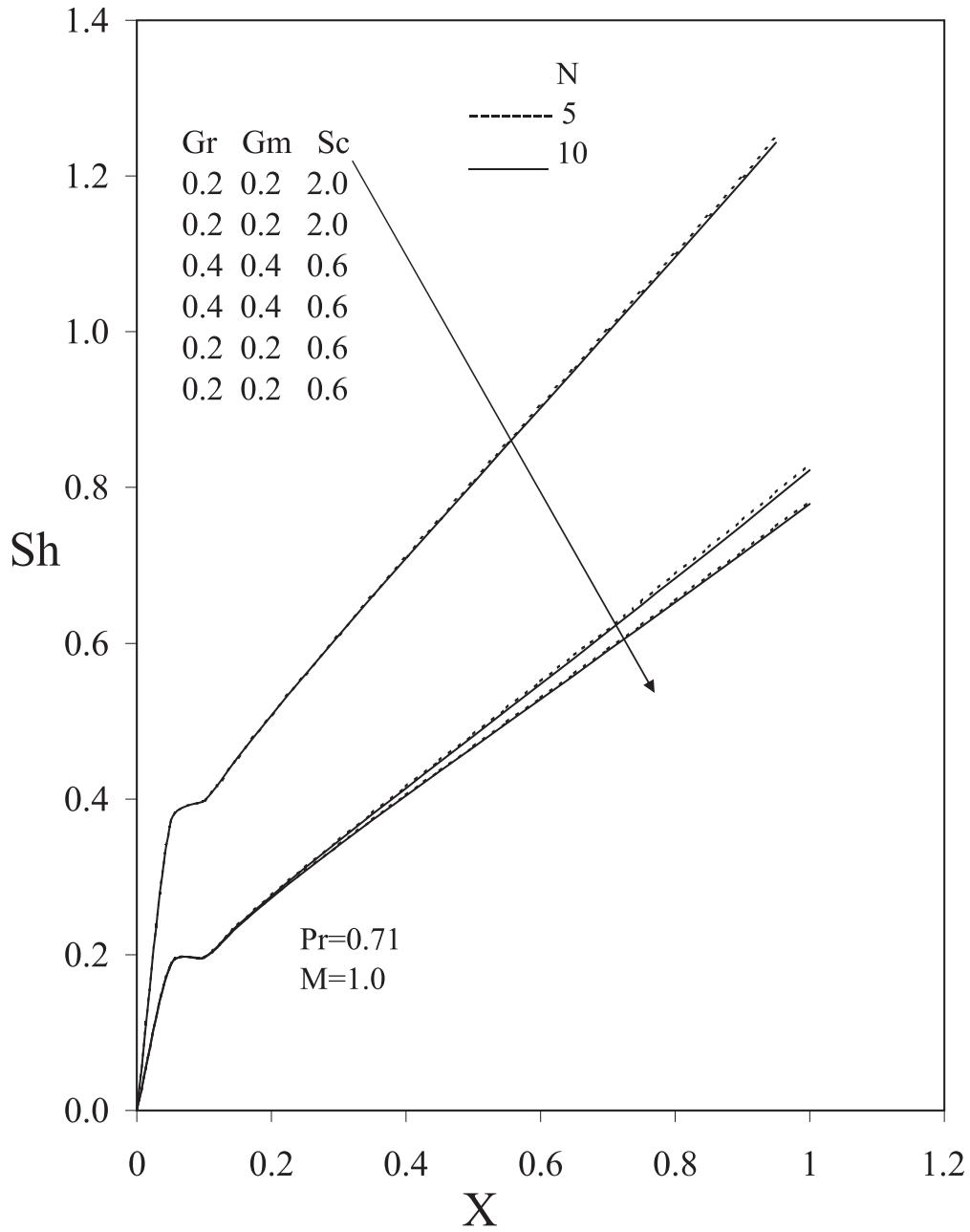


Figure 15: Local Sherwood number.



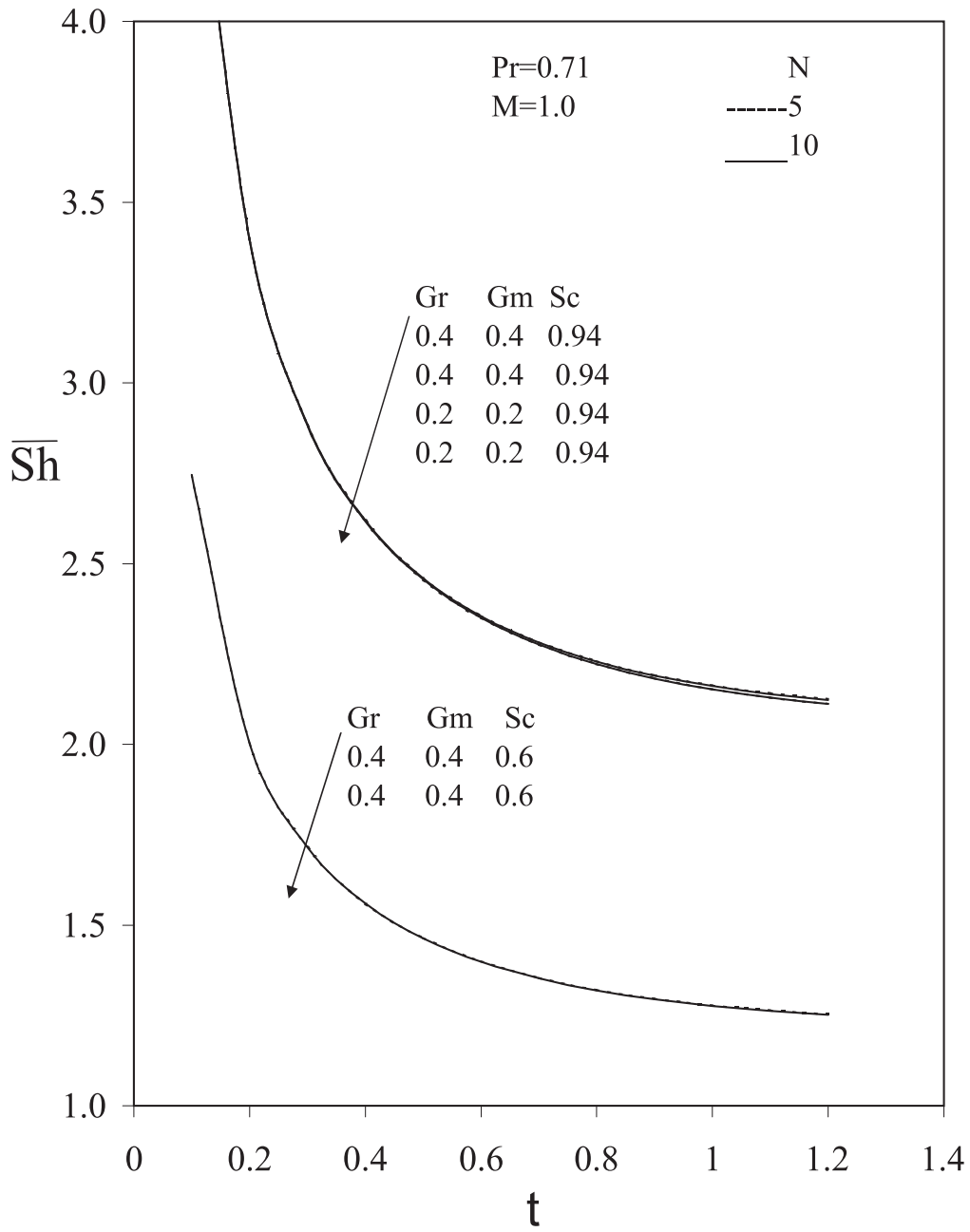


Figure 16: Average Sherwood number.